*Laser and Particle Beams* (2003), *21*, 139–156. Printed in the USA.

DOI: 10.1017/S0263034603212039

# Current status of plasma emission electronics: II. Hardware

A.S. BUGAEV,[1] A.V. VIZIR,[1] V.I. GUSHENETS,[1] A.G. NIKOLAEV,[1] E.M. OKS,[1] G.YU. YUSHKOV,[1] YU.A. BURACHEVSKY,[2] V.A. BURDOVITSIN,[2] I.V. OSIPOV,[2] AND N.G. REMPE[2]

[1]Institute of High Current Electronics, Siberian Division of the Russian Academy of Science, Tomsk, Russia
[2]State University of Control Systems and Radioelectronics, Tomsk, Russia

(RECEIVED 1 April 2003; ACCEPTED 16 May 2003)

**Abstract**

This paper is devoted to the engineering embodiment of the modern methods for producing charged ion and electron beams by extracting them from the plasma of a discharge. Electron beams use to execute electron-beam welding, annealing, and surface heating of materials and to realize plasmochemical reactions stimulated by fast electrons. Ion beams allow realization of technologies of ion implantation or ion-assisted deposition of coatings thereby opening new prospects for the creation of compounds and alloys by the method that makes it possible to obtain desired parameters and functional properties of the surface. A detailed description is given to the performance and design of devices producing beams of this type: the ion and electron sources being developed at the laboratory of plasma sources of the Institute of High-Current Electronics of the Russian Academy of Sciences and the laboratory of plasma electronics of Tomsk State University of Control Systems and Radioelectronics.

**Keywords:** Discharge; Electron or ion beam; Electron or ion source; Plasma

## 1. INTRODUCTION

The technologies based on the action of accelerated charged particle beams on the surface of various materials constitute one of the most promising and intensely developing fields of modern industry. Electron beams can be used to execute electron-beam welding, annealing, and surface heating of materials and to realize plasmochemical reactions stimulated by fast electrons. Ion beams allow realization of technologies of ion implantation or ion-assisted deposition of coatings, thereby opening new prospects for the creation of compounds and alloys by the method that makes it possible to obtain desired parameters and functional properties of the surface. The appearance of this field of applications gave rise to a new class of technological electron and ion sources that feature a simple design, reliability, high productivity, and comparatively low cost. Extensive research in this field calls for continuous improvement of the existing systems and creation of conceptually new charged particle sources. On the other hand, the better performance and the broader spectrum of their functional capabilities open new fields of applications for these technologies. It is expected that in the near future, a number of new industrial operations in which a charged particle beam is the main tool will appear.

This article is devoted to the engineering embodiment of the modern methods for producing charged particle beams by extracting them from the plasma of a discharge. (The physical foundations of these methods are discussed in the article by Gushenets *et al*., 2003, in this issue.) A detailed description is given to the performance and design of devices producing beams of this type: the ion and electron sources being developed at Institute of High-Current Electronics of the Russian Academy of Sciences and the laboratory of plasma electronics of the Tomsk State University of Control Systems and Radioelectronics.

## 2. PLASMA ELECTRON SOURCES

### 2.1. Accelerators and sources of electrons with a plasma emitter based on a low-pressure arc discharge of microsecond duration

The principal method for the formation of pulsed electron beams in plasma-emitter electron sources and accelerators is "modulation" of the discharge current. This is the simplest

Address correspondence and reprint requests to: Dr. Alexey G. Nikolaev, High Current Electronics Institute, 4 Akademichesky Ave., 634055 Tomsk, Russia. E-mail: nik@opee.hcei.tsc.ru

and widely used technique. The beam current pulse duration and the pulse repetition rate are determined by the pulse duration and repetition rate of the discharge current. For a low-operating-voltage arc discharge, this makes it possible to attain high energy efficiency of the plasma emitter, as compared to hot emitters. Once the discharge has been initiated, plasma fills the hollow anode whose size is determined by the cross-sectional area of the electron beam. The time it takes for the discharge plasma to fill this cavity, or the plasma formative time, depending on the cavity volume, the working pressure of the plasma-generating gas, and some other factors, is at most a few microseconds (Koval *et al.*, 1983). The plasma generation process is responsible for the rise time of the emission current, and the plasma decay in the cavity determines the fall time of the electron current. Thus, both processes are responsible for the time and frequency parameters of the pulsed electron beam. The first process limits the rise time and the minimum pulse duration of the electron beam current, while the second one limits the maximum pulse repetition rate. The emission current amplitude and density are restricted in the main by the electric strength of the acceleration gap.

Figure 1 presents a schematic diagram of one of the series of electron sources and accelerators with modulation of the discharge current (Belyuk *et al.*, 1983; Gushenets *et al.*, 1986; Vintizenko *et al.*, 1986, 1988; Gavrilov *et al.*, 1993; Gielkens *et al.*, 1996), which was used to perform the first experiments on the production of high-current electron beams. With this device, the shortest possible electron beam pulse durations have been achieved with a rather high efficiency and emission current pulses of stable waveform and amplitude. The plasma emitter consists of a hollow cylinder

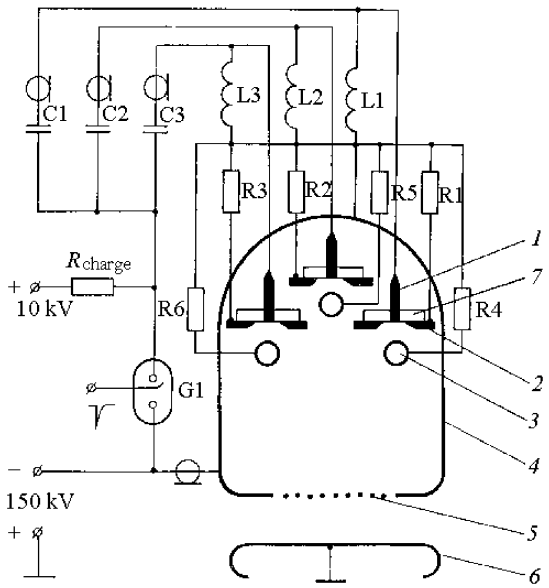


**Fig. 1.** Schematic of a plasma-emitter electron source: *1*: cathode, *2*: trigger electrode, *3*: dissipating electrode, *4*: hollow anode, *5*: emission grid, *6*: collector, and *7*: insulator.

(hollow anode *4*) 20 cm in diameter and length with three plasma generators mounted inside the cylinder. Each generator consists of cathode *1*, trigger electrode *2*, and insulator *7*. The use of three plasma generators is dictated by the need to meet the requirements of lifetime (over $10^7$ pulses) and a uniform current density distribution over the electron beam cross section. The latter is also attained with the help of spherical electrodes *3*. In some design versions, the number of plasma generators varied from two (Gielkens *et al.*, 1996) to seven (Belyuk *et al.*, 1983). A rather detailed description of these plasma generators is given elsewhere (Gilmour & Lockwood, 1972). They are simple in design and, in contrast to the plasma generators based on a constricted arc (Gavrilov *et al.*, 1993) and a glow discharge (Rempe *et al.*, 2000; Volkov *et al.*, 2001), have, in fact, no limitation on the maximum discharge current. This advantage makes them attractive for use in high-current electron sources. On the end face of the hollow anode, extraction window *5*, covered with a fine grid, is mounted. The accelerating voltage is, as a rule, steady; its magnitude being up to 150 kV, it is applied between the hollow anode and collector *6*.

Once an arc has been initiated, due to the breakdown of dielectric *7*, a discharge is ignited between the hollow anode and cathode *1*. In the experiments described in Koval *et al.* (1985), two discharge ignition and operation modes, conventionally named the vacuum mode and the gas mode, were observed. Both modes feature a rather low working pressure at which the mean free path of electrons for the reaction of ionization is much greater than the electrode gap spacing. However, when the pressure is over some critical value $p_{cr}$, which can be estimated by the formula (Kozyrev *et al.*, 1994)

$$N_{cr} = \frac{6}{\pi}\left(\frac{m}{M}\right)^{1/2}\frac{1}{\sigma_i d}, \qquad (1)$$

the residual gas in the discharge gap has a noticeable effect on the discharge ignition and operation. The generally accepted idea is that the generation of plasma inside the anode cavity in the vacuum mode occurs due to the cathode plasma expanding into the gap between the cathode and anode. This mode is most often used in metal-ion sources; however, it can also be harnessed in highly efficient electron sources with stringent requirements on the vacuum conditions. The disadvantage of this operating mode is the rather unstable pulse of the electron emission current. This is related to the fact that, because of the unstable nature of the cathode spot, plasma and vapors enter the anode cavity nonuniformly. This is illustrated by the oscillograms of the electron beam current (see Fig. 2a) recorded for a discharge operating in the "vacuum" mode at a pressure of nitrogen gas supplied into the discharge chamber of the plasma emitter of $10^{-4}$ Torr.

An increase in gas pressure has the result that some of the electrons emitted from the boundary of the plasma blob (flare) formed at the cathode ionize the gas. Thus, at a pressure $p > p_{cr}$, another mechanism for plasma production

https://doi.org/10.1017/S0263034603212039 Published online by Cambridge University Press

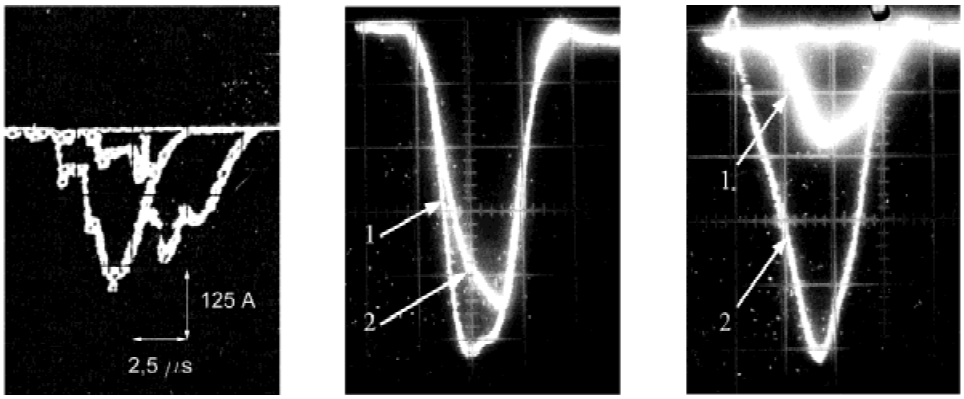


**Fig. 2.** Oscillograms of the emission current (a, b, c) and the discharge current (trace *2* in c). Horizontal scale for b and c: 1 $\mu$s/div; vertical scales: 200 A/div (b), 500 A/div (c).

comes into play, and, in some cases, this mechanism appears to be faster than the mere expansion of the cathode flare plasma, and the discharge ignition time shortens. This is the best mode for a plasma electron emitter. With a discharge operating in this mode, the electron beam produced has a highly stable current pulse waveform and amplitude and a uniform current density distribution over the beam cross section. Figure 2c presents the waveforms of 10 emission current pulses recorded sequentially (waveform *1*). In accordance with formula (1), the use of a gas with a high molecular weight for the working gas makes it possible to reduce the working pressure, which is observed in experiments. Filling the working chamber with Xe not only reduces the working pressure, but also improves the emission current waveform, as can be seen in Figure 2c that gives the emission current waveforms recorded for the operation with Xe (*1*) and $N_2$ (*2*).

For the investigated pressure range $1\cdot10^{-4} - 4\cdot10^{-4}$ Torr, there occurs in the main a diffuse discharge between the cold cathode and the internal surface of the hollow anode, which is sometimes disrupted by the anode spots formed at the cavity surface. The probability of the appearance of these spots depends on the condition (degree of contamination) of the anode internal surface as well as on the fill gas pressure and the discharge current amplitude and duration. Experience on plasma emitters shows that this problem can be resolved by using oil-free pumping and properly choosing the material for the hollow anode electrodes. The replacement of the aluminum parts of the hollow anode by parts made of stainless steel has made it possible to increase the discharge current to 3–3.5 kA without formation of anode spots.

Based on the results of experimental investigations performed with this plasma-emitter electron source, a series of high-current electron accelerators had been developed that were used in the main in experiments on the production of laser radiation (Vintizenko *et al.*, 1986, 1988; Gavrilov *et al.*, 1993; Galansky *et al.*, 1994; Gielkens *et al.*, 1996). Figure 3 presents a schematic diagram of an accelerator for the production of an electron beam of cross-sectional area $15 \times 60$ cm$^2$ (Vintizenko *et al.*, 1986). This accelerator was used in experiments on the generation of laser radiation in inert gases. The plasma emitter includes common cylindrical anode *1*, on the end faces of which are two cathode assemblies of the discharge system. The plasma-generating gas (nitrogen or argon) was supplied into the discharge gap (hollow anode cavity) to a working pressure of $2\cdot10^{-2}$ Pa. On the side surface of the hollow anode, an extraction window, covered with a fine grid, is mounted. The window dimensions determine the cross-sectional area of the beam. The extraction and acceleration of electrons is executed by a dc voltage applied between the hollow anode and the vacuum chamber. When the beam is extracted into the atmospheric air or high-pressure gas through a thin foil, a dc voltage minimizes the electron losses and makes it possible to produce a nearly monoenergetic beam because there is no ac-

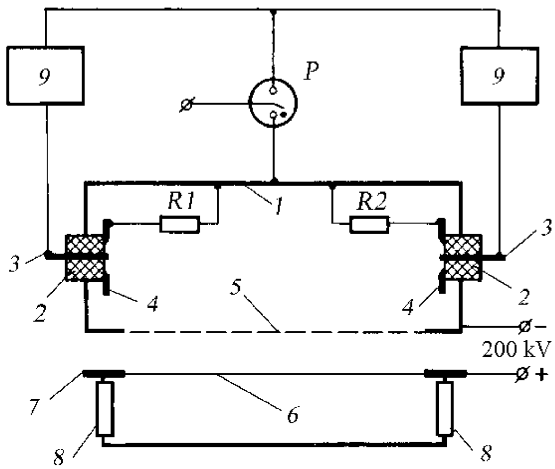


**Fig. 3.** An electron accelerator with a rectangular beam cross section (Vintizenko *et al.*, 1986): *1*: hollow anode, *2*: insulator, *3*: cathodes, *4*: trigger electrodes, *5*: emitting grid, *6*: Al foil, *7*: support electrode, *8*: laser mirrors, *9*: pulse forming lines, P: gas switch, and *R1*, *R2*: resistors.

https://doi.org/10.1017/S0263034603212039 Published online by Cambridge University Press

celeration of electrons during the high voltage pulse rise time and fall time.

When an electron beam is used for pumping gas lasers, its important characteristic is the uniformity of the current density distribution over the beam cross section, which is responsible for both the efficiency of using the beam and the probability of breakdown in the active mixture of the laser if the beam has a local nonuniformity. The method for improving the beam current density distribution is based on the dependence on the electron emission on the proportion between the mesh size of the grid and the width of the negative potential fall near the grid. To make the cross-sectional beam current density distribution more uniform, a varied-transparency grid was mounted in the extraction window. Another way of improving the current density distribution is to change the inclination angle $\gamma$ (Gielkens *et al.*, 1996; Fig. 4) of the cathode assembly with respect to the axis of the hollow anode.

With an accelerating voltage of 150–200 kV, a pulse repetition rate of 50 $cm^{-1}$, and pulse duration of 30 $\mu$s, an electron beam with a current of up to 50–80 A has been produced. The beam was extracted into a laser cell through 30-$\mu$m aluminum-beryllium foil. With a 70% geometric transparency of the support grid, which is cooled with water on its periphery, the extracted current makes up 50% of the beam current in the acceleration gap. When operated in the single-pulse mode, the accelerator produced a beam with a current of up to 1000 A at a pulse duration of 5–10 $\mu$s, up to 400 A at a pulse duration of 15 $\mu$s, up to 200 A at a pulse duration of up to 30 $\mu$s, and at a pulse duration of up to 100 $\mu$s, the peak current of the beam was 25–90 A.

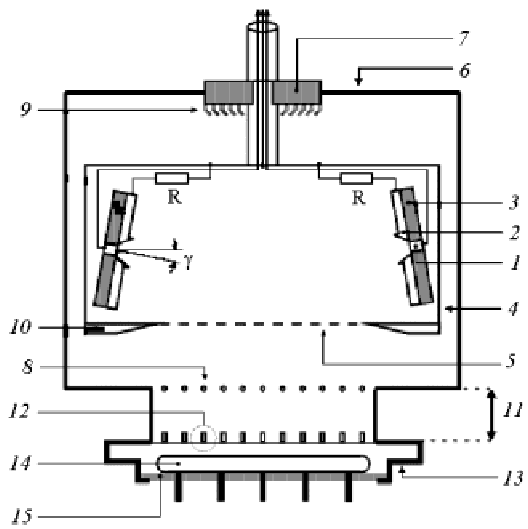


**Fig. 4.** Schematic drawing of the gun (Gielkens *et al.*, 1996): *1*: discharge cathode, *2*: intermediate electrode, *3*: insulator, *4*: hollow anode, *5*: extraction grid, *6*: vacuum chamber, *7*: high-voltage insulator, *8*: grid anode, *9*: voltage gradient rings, *10*: field shaping electrode, *11*: drift section, *12*: Ti foil window and support structure, *13*: laser chamber, *14*: discharge electrode, and *15*: insulator.

An electron accelerator for which the beam current pulse duration was determined by the pulse duration of the accelerating voltage rather than by the discharge ignition and operation times is described elsewhere (Gielkens *et al.*, 1996). A schematic diagram of the accelerator is given in Figure 4; oscillograms of the discharge current, accelerating voltage, beam current, and collector current behind the foil are presented in Figure 5. In the absence of an accelerating voltage, the discharge plasma comes from the hollow anode into the acceleration gap and fills the latter. As an accelerating voltage is applied to the gap, it is localized across a narrow region adjacent to the emission grid. This results in an increase in electric field near the grid electrode, and, as the electric field reaches a certain value, emission centers appear on the grid surface. Dense plasma appears near the emission grid and, propagating toward the extraction grid, bridges the gap. This is a possible mechanism for the breakdown of the acceleration gap. The length of this region, with the accelerating voltage amplitude and rise time being the same, is determined by the density of the penetrating plasma. The plasma density depends on the magnitude of the discharge current in the discharge system, the mesh size of the grid, and the time delay to the discharge initiation relative to the application of the accelerating voltage. This time delay also affects the waveform of the voltage across the acceler-

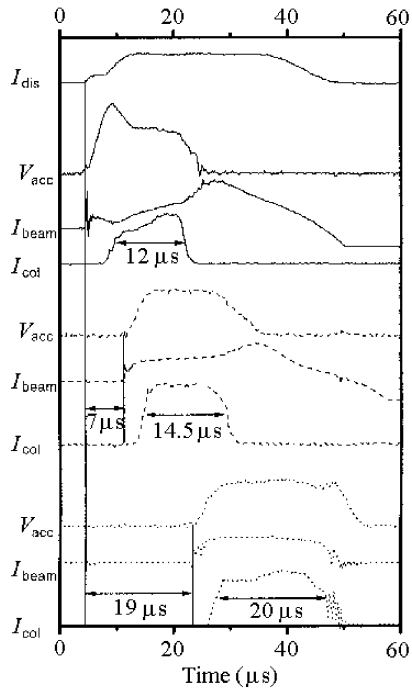


**Fig. 5.** Waveforms of the discharge current $I_{dis}$, the accelerating voltage $V_{acc}$, beam current $I_{beam}$, and collector current $I_{col}$. When the accelerating voltage and discharge current start simultaneously, the beam current rises only slowly (solid curves). With sufficient delay, the beam current rises immediately (dashed curves). Finally, by adjusting the falling slopes of the discharge current and accelerating voltage it is possible to eliminate the high-voltage discharge at the end of the pulses (dotted curves).

https://doi.org/10.1017/S0263034603212039 Published online by Cambridge University Press

ation gap, as the voltage pulse generator has a finite internal resistance, and the waveforms of the beam and collector currents (Fig. 5). By properly choosing the mentioned parameters, stable operation of the accelerator was attained with the beam current equal to 270 A at a peak accelerating voltage of 200 kV; the collector current pulse duration was 15–20 $\mu$s; the beam electron losses in the extraction grid and the foil made up 65%.

A new application of the plasma electron emitter is its use for increasing the mean charge of the ion beam in an ion source based on a vacuum arc operating in the vapor of the cathode material (MEVVA). Injection of a low-energy electron beam into plasma increases the ion charge (Bugaev *et al.*, 2001). In the above electron accelerators, the discharge operated in the hollow anode of the electron emitter at a pressure of $3\cdot10^{-2}$ Pa, which was over the critical pressure $p_{cr}$ for the given geometric dimensions. At this pressure, a discharge resembling a gas discharge is initiated in the discharge gap, and gas-discharge plasma is generated. Experimental investigations of the charge state of the ion beam (Oks & Yushkov, 1996) extracted from an ion source with the discharge gap geometry similar to those described above have shown that, as the pressure is increased to above $2\cdot10^{-2}$ Pa, the percentage of metal ions (of the cathode material, e.g., Al) decreases to 20% and even to lower values, while 80% of the ion beam are the ions of the gas filling the discharge gap. This relatively low pressure stabilizes the emission current in an electron source, but it is entirely unacceptable in metal ion sources. It has been demonstrated (Spadtke *et al.*, 1994) that the mean charge of metal ions noticeably decreases even when the pressure is over $6\cdot10^{-4}$ Pa.

A plasma electron emitter (Bugaev *et al.*, 2000*a*) based on a vacuum arc with an emission current density of 20–40 A/cm$^2$, which operates under the conditions of high vacuum ($p \leq 2\cdot10^{-4}$ Pa) and features high efficiency of electron extraction (Nazarenko *et al.*, 1987), has been developed for the use in an ion source with an electron beam (E-MEVVA). The experimental mockup of a plasma-emitter-based electron gun on which the electron source design was tried out is given in Figure 6. The principal units of the mockup are the plasma emitter and the electron beam focusing system. The plasma emitter is formed by cold cathode *1*, hollow anode *2*, and trigger electrode *3*. On one of the end faces of the hollow anode there is emission window *5* of diameter 1.5 cm, covered with a fine grid. The plasma emitter is completely immersed in the longitudinal magnetic field (0.1–0.2 T) of solenoid *12*. The beam transportation and focusing is executed in channel *6*, inside of which plasma generator guns are installed. The extraction electrode is made as a disk with a hole of diameter 1.8 cm, not covered with a grid. To compensate the defocusing effect of the transverse electric field in the hole of the extraction electrode and that of the electron beam space charge, the transportation channel and the space within this hole were filled with plasma, produced by the plasma generators, and the system was immersed in the magnetic field of solenoid *13*. At the exit of the transportation channel, focusing coil *14* is placed. The maximum magnetic field at the coil axis reaches 1 T.

In the course of the experiment, an electron beam of current up to 80 A was produced at a pulse duration of up to 100 $\mu$s and an accelerating voltage of 20 kV. Oscillograms of the emission and collector currents and the autograph of the beam on the collector are shown in Figure 7. The current density at the collector was 25–30 A/cm$^2$, while the current density in the hole of diaphragm *10* reached 160 A/cm$^2$.

The collector plasma and the collector material vapor had an insignificant effect on the electric strength of the acceleration gap because of the fact that only a small fraction of them penetrated, through the hole in the focusing coil, into the transportation channel and then into the acceleration gap. This electron source design is a candidate for technologies where an electron beam is used for pulsed melting of metal surfaces to modify their properties.

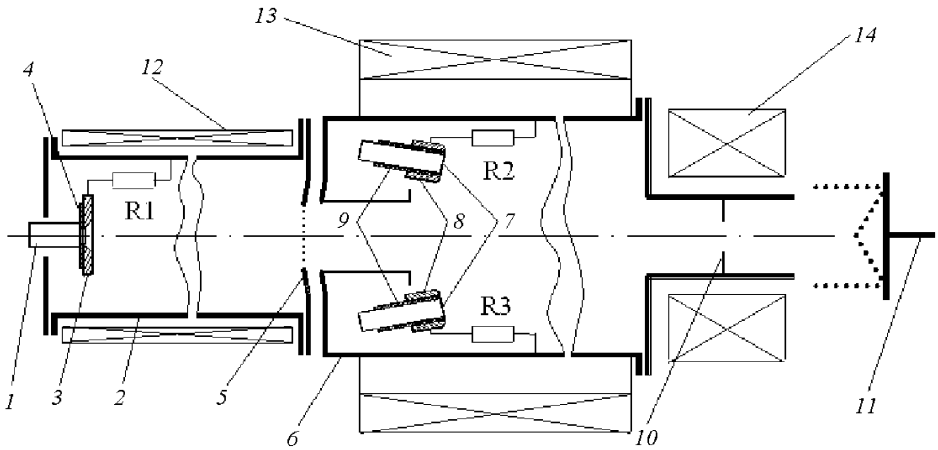


**Fig. 6.** Schematic drawing of the electron gun (Bugaev *et al.*, 2000*a*): *1*, *7*: cathodes, *2*: hollow anode, *3*, *8*: trigger electrodes, *4*, *9*: insulators, *5*: emitting electrode, *6*: transport channel, *10*: diaphragm, *11*: collector (Faraday cup or plate), and *12*, *13*, *14*: coils.

https://doi.org/10.1017/S0263034603212039 Published online by Cambridge University Press

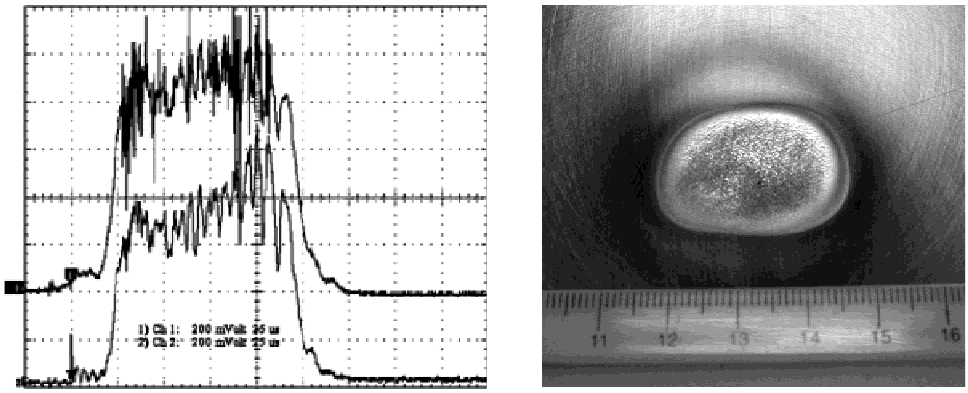

**Fig. 7.** The left figure shows waveforms of collector (upper trace) and emission currents (lower trace). Vertical scale: 20 A/div, horizontal scale: 25 $\mu$s/div. The right figure presents an electron beam autograph (about 50 J/cm$^2$).

A slightly modified version of the electron source was employed in experiments on increasing the mean charge in MEVVA-type ion sources (Bugaev *et al.*, 2001).

### 2.2. Nanosecond pulsed electron sources

The time of plasma formation in the anode cavity of a plasma emitter strongly depends on the background or plasma-generating pressure and, at a very low pressure, it is determined by the plasma expansion velocity, which is approximately equal to $10^6$ cm/s. In this connection, for the electron emitters designed for the production of electron beams with a cross-sectional area of tens of centimeters, the rise time of the emission current may be some tens of microseconds. The grid control method makes it possible to produce pulsed electron beams with desired time characteristics (pulse rise time and fall time), which may be many times shorter than the plasma formative time.

Figure 8 presents a schematic diagram of a grid-controlled plasma electron emitter (Bugaev *et al.*, 1992*a*) in which, as in the emitters described above, the emitting plasma is produced due to an arc discharge operating between cathode *1* and hollow anode *5* both in the cathode material vapor and in the gas supplied into the anode cavity through a controllable leaker. The optimum pressure of the fill gas lies in the range from $10^{-2}$ to $3\cdot10^{-2}$ Pa. To lengthen the emitter lifetime and improve the beam uniformity, seven initiating systems were used which had, correspondingly, seven cathodes and seven trigger electrodes. Each cathode was connected to an individual artificial pulse-forming line. All trigger electrodes were connected through resistors of rated resistance 50–100 Ω to the hollow anode. A negative dc voltage of up to 100 V was applied to emission grid electrode *8*, insulated from the hollow anode, which practically prevented the plasma electrons from entering the acceleration gap between the emission electrode and collector *9*. An accelerat-

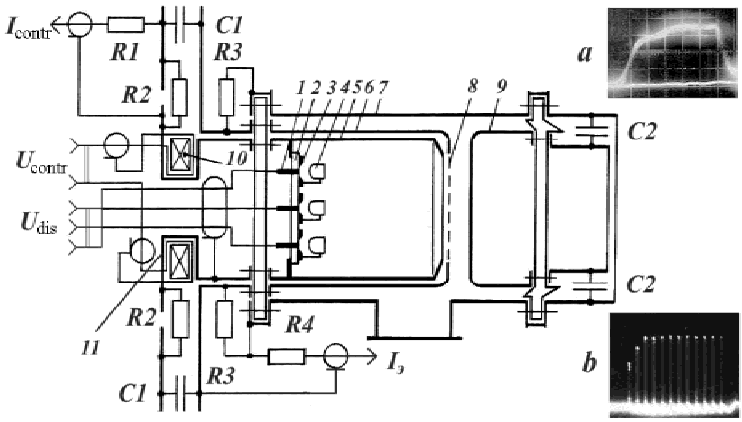


**Fig. 8.** Plasma electron emitter with grid control: *1*: cathode, *2*: insulator, *3*: trigger electrode, *4*: redistributing electrode, *5*: hollow anode, *6*: control electrode, *7*: vacuum chamber, *8*: emitting grid, *9*: collector, *10*: pulse transformer, and *11*: second winding of the pulse transformer. Oscillograms: waveform of emission current pulse (a, vertical scan is 210 A/div, sweep is 20 ns/div) and 12-pulse burst with 33 $\mu$s delay (b).

https://doi.org/10.1017/S0263034603212039 Published online by Cambridge University Press

ing dc voltage was applied between the emission electrode and the collector. As the hollow anode was filled with plasma, positive pulses were applied to the emission grid from a nanosecond voltage pulse generator, resulting in lowering the potential barrier near the grid and in the appearance of an emission current. To attain better time characteristics, the pulsed transformer of the generator was integrated with the plasma emitter. An oscillogram of 10 superimposed pulses of the electron beam current is given at the upper right of Figure 8. It can be seen that the pulses almost follow one another in waveform and amplitude, demonstrating the high stability of the plasma emitter. The maximum peak current of the collector reached 700–800 A at a discharge current of 1300 A, a pulse duration of 100 ns, and a rise time of 25–30 ns.

Further increase in emission current was prevented by the breakdown between the grid and the hollow anode that occurred even at a negative voltage at the grid. The occurrence of breakdowns is associated with the charging of the dielectric inclusions present in the surface layer of the grid by the ion current from the plasma. As the charge on these inclusions reaches a certain value, there occurs flashover with the formation of a cathode spot on the grid, which is followed by the initiation of an arc discharge between the hollow anode and the grid. A solution of this problem would make it possible to increase the emission current, since there are no conceptual limitations on the discharge current.

The plasma emitter under consideration is designed to be integrated with a linear induction accelerator. It is capable of operating in a repetitive packet mode with a packet length of about 1 ms and an interval between electron beam current pulses within a packet of 30–33 $\mu$s.

Based on the results of investigations of the grid-controlled electron emitter, an electron accelerator has been developed and built to perform experiments on the production of laser radiation (Gushenets *et al.*, 1991). This generator, like its prototype, operates in the repetitive packet mode with a packet length of 200 $\mu$s and a pulse repetition rate in a packet of up to $4\cdot10^5$ s$^{-1}$. A schematic diagram of the accelerator is given in Figure 9. Emitter *3* is mounted, with the help of bushing insulator *8* and a current lead, in vacuum chamber *9*. Plasma is produced by four cathode assemblies *1* with arc discharges that are initiated on application of a voltage from pulse-forming lines connected to the output stage of a VPG. The pulsed current of a discharge of duration 200 $\mu$s is controlled in the range from 0.3 to 1 kA. A dc negative bias $U_{bias}$ of 400 V is applied between hollow anode *2* and emission grid *4*. Bell-shaped positive-polarity pulses $U_{contr}$ of FWHM 170 ns and amplitude 3 kV are supplied from the generator through pulsed transformer *7* mounted in the body of insulator *8*. With an accelerating voltage of 160 kV, a discharge current of 400 A, a 70% geometric transparency of the support grid, and a 18-$\mu$m-thick titanium foil, a beam of current 100 A and a cross section of $3 \times 70$ cm has been extracted into the laser cell. Estimates show that in an accelerator with the emission

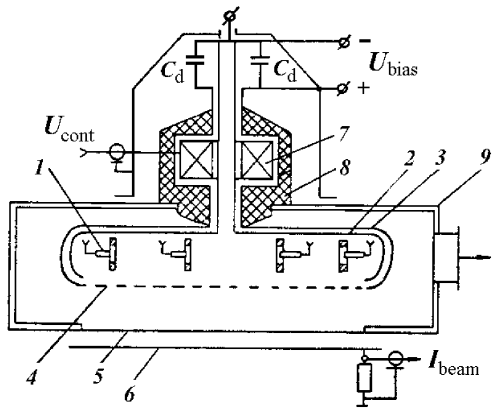


**Fig. 9.** Schematic drawing of an accelerator with a high pulse repetition rate (Belyuk *et al.*, 1983): *1*: cathode unit, *2*: hollow anode, *3*: outer cylindrical electrode, *4*: emitting control grid, *5*: Ti foil with support structure, *6*: collector, *7*: pulse transformer, *8*: bushing insulator, and *9*: vacuum chamber.

current controlled by a grid, the pulse repetition rate can be increased to a few megahertz.

The arc-discharge plasma electron emitters have a considerable disadvantage: They have short lifetimes. This is related to the fact that the operation of the arc discharge results in significant erosion of the cathode, leading to an increase in gap spacing between the cathode and the trigger electrode, and with time the discharge initiation becomes ineffective. In some cases, the cathode material deposited on the surface of the insulator separating the cathode and the trigger electrode, and the electrodes closed to one another. This disturbed normal operation of the emitter. The lifetime of this type of emitter is $\geq 10^7$ pulses. Therefore, plasma electron emitters have been developed that depend for their operation on a glow discharge with a hollow cathode (Gushenets *et al.*, 1999), whose lifetime is $10^9$ or even more pulses. Figure 10 presents a schematic diagram of an electron source with a glow-discharge emitter. The source consists of hollow anode *3* of diameter 20 cm and length 75 cm on the ends of which two plasma generators are mounted which supply plasma into the anode. The plasma generators are joined with the anode through small (5 mm in diameter) holes where a pressure difference is realized, so that the pressure in the plasma generators is at least an order of magnitude greater than that in the anode. The operating pressure in the anode cavity is generally not above $5\cdot10^{-2}$ Pa, and for the plasma-producing gas nitrogen or air is generally used. Each of the plasma generators consists of hollow cathode *1* and intermediate electrode *2*. To increase the lifetime of the system, a glow discharge is used in the plasma generators as well. A magnetic field of 0.3 T, which is created by permanent ring-shaped magnets, reduces the ignition voltage of the discharge and the operating pressure in the plasma generators and provides low-jitter discharge ignition.

The discharge system of the emitter operates as follows: First an igniting hollow-cathode discharge is initiated in the

https://doi.org/10.1017/S0263034603212039 Published online by Cambridge University Press

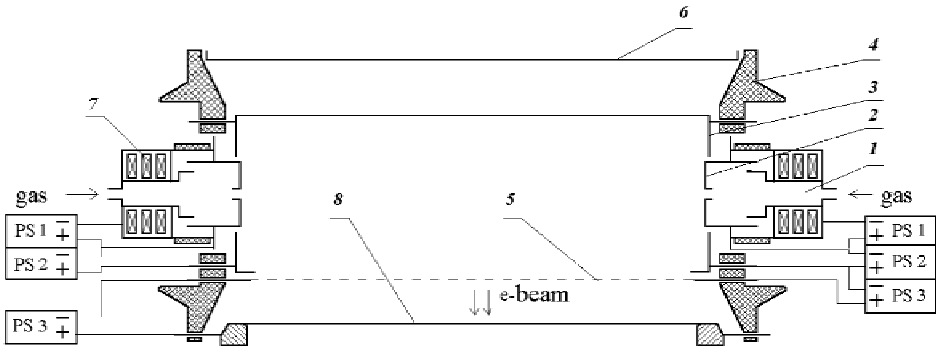


**Fig. 10.** Schematic of a glow-discharge electron source: *1*: plasma generator cathode, *2*: intermediate electrode, *3*: hollow anode, *4*: insulator, *5*: emission electrode, *6*: vacuum chamber, *7*: magnets, and *8*: collector.

magnetic field between electrodes *1* and *2* and then, after a time, a voltage is applied between electrodes *2* and *3*, initiating a discharge with a hollow cathode, the latter being intermediate electrode *2*.

The currents of the igniting discharge between cathode *1* and electrode *2* and of the auxiliary discharge between electrode *2* and anode *3*, the durations of their pulses, and the time delay of the ignition of the auxiliary discharge relative to the igniting discharge were chosen in the course of experimental investigations, proceeding from the condition that the hollow anode should be filled with plasma uniformly. The pulse amplitude and duration of the igniting discharge current were, respectively, 30 A and 10–12 $\mu$s; for the auxiliary discharge current, these quantities were 60–70 A and 14–16 $\mu$s; the time delay between the discharges was 6–8 $\mu$s. With a shorter time delay and a lower current of the igniting discharge, the plasma in the hollow anode is shaped as a filament unstable in space and in time. A pulsed voltage of up to 10–12 kV was applied, with a delay of 6–10 $\mu$s relative to the ignition of the auxiliary discharge, between the hollow anode and emission electrode *5*, covered with a 70% transparency grid. In the absence of this voltage, the current was lower by almost two orders of magnitude due to the negative voltage that appeared at the grid as the electron current passed through the internal resistance of the (open) switch of the nanosecond pulse generator.

Under experimental conditions, the pulse rise time of the current onto the emission electrode and collector *8* was determined by the rise rate of the applied voltage. The waveform of the pulse top depended on the time delay of the voltage application to the grid relative to the ignition of the auxiliary discharge. As the delay was decreased, the slope of the current pulse waveform increased at the top, while the current within the pulse rise time decreased. The maximum emission current achieved in experiment was 140 A at an accelerating voltage between the grid electrode and the collector of up to 30 kV (Fig. 11). The current pulse rise time was 25–30 ns. The efficiency of electron extraction, which is equal to the emission-to-discharge current ratio, is proportional to the transparency of the grid emission electrode $\eta$, that is, $I_e = \eta I_p$. The current density distribution along the major axis of the beam cross section was uniform to within ±15%.

Later this plasma emitter was modified (Gushenets & Schanin, 1999), which made it possible to do away with one plasma generator and thus substantially simplify the emitter design.

### 2.3. Plasma-emitter electron sources for the production of focused continuous electron beams

A number of industrial electron-beam technologies are based on the use of continuous and pulsed electron beams of small cross section with a high power density (Belyuk *et al.*, 1983; Nazarenko *et al.*, 1987). The electron sources that are operated in industry should provide reproducible parameters of the electron beam for a long time (Nazarenko *et al.*, 1987). Under high vacuum, stabilizing the source parameters is not a particular problem. However, under actual conditions of industrial production, there are a number of destabilizing factors such as “commercial” vacuum, the directed vapor-gas flow from the melt region, and often losses of pressure, including emergencies, in the working chamber of the system. When operated under these conditions, plasma-emitter electron sources, having no hot cathode, offer the opportunity to keep the electron beam parameters invariable by

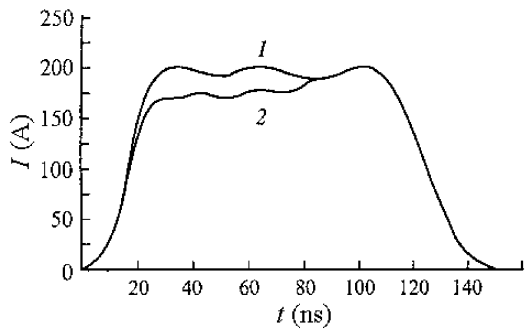


**Fig. 11.** Oscillograms of the current in the circuit of emission grid electrode *5* for a delay time of 10 (*1*) and 6 $\mu$s (*2*).

https://doi.org/10.1017/S0263034603212039 Published online by Cambridge University Press

simpler means than hot-cathode sources. This gave impetus to the development of plasma-emitter electron sources, which could be used in electron-beam technologies.

The required plasma-emitter electron sources have been developed based on a hollow-cathode reflected discharge (Galansky *et al.*, 1994; Rempe & Osipov, 2000; Rempe *et al.*, 2000). Various design versions of plasma-emitter electron sources have been developed for use under the conditions of industrial production.

Figure 12 presents a schematic diagram of the discharge chamber of an electron source. The base of the discharge chamber and of the source as a whole is a welded cermet unit consisting of high-voltage ceramic insulator *1* with rings *2* and anode assembly *3*, welded to the insulator. The anode assembly contains bearing cermet insulators *4* welded to the anode of discharge chamber *5*. Dismountable hollow cathode *6* is mounted on the central bearing insulator; the remaining insulators are intended to fix cooling radiator *7* of cathode *8* with an emission hole and the electric insulation of the cathode. Cathode *8* is dismountable and it has a channel for electrons to go from the discharge chamber into vacuum. Dismountable magnet *9* creates a magnetic field of induction of about 0.01 T in the discharge chamber.

The discharge chamber electrodes can heat up in the course of prolonged continuous operation of the source. In this connection, a source is furnished with a cooling system. With low (below 100 mA) currents, the cooling occurs due to the convection of the transformer or castor oil filling the source cavity. If necessary, forced cooling of the oil can be accomplished with the use of a water coat in the source case.

The source is equipped with is a system for dosed gas supply. The working gas enters the discharge chamber, through a leaker, which controls gas supply, and the hollow cathode channel, via dielectric tube *10*.

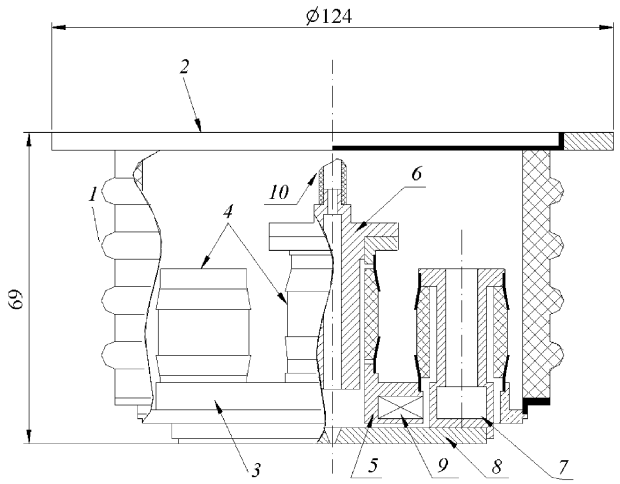


**Fig. 12.** A plasma-emitter electron source: *1*: ceramic high-voltage insulator, *2*: insulator gaskets, *3*: anode assembly, *4*: bearing insulators, *5*: anode, *6*: hollow cathode, *7*: cooling system, *8*: cathode with an emission hole, *9*: permanent magnet, and *10*: working gas supply.

The plasma-emitter electron sources have found the widest industrial use in welding technologies. They are employed in flow lines for sealing fuel elements of nuclear power stations (Volkov *et al.*, 2001). In fuel elements, the fuel is encapsulated in a sealed-off thin-wall metal can. The tightness of the can is the key factor that is responsible for the operability of a fuel element operated in a nuclear reactor. The can of a fuel element should remain intact throughout its service life, which, depending on the type and operating conditions of the fuel element, may be as long as several years.

Fuel element cans are made primarily of zirconium or aluminum alloys. Zirconium and its alloys are highly reactive toward oxygen, nitrogen, and hydrogen. In view of this, when sealing a fuel element, it is of importance to afford good protection of the welding zone. This protection is ensured by welding zirconium in vacuum at a pressure not over $10^{-3}$ Pa. The welding of aluminum alloys can be performed at a higher pressure of the residual gas in the vacuum chamber.

Electron sources of this type are operated on automatic flow lines. Continuous production places stringent requirements upon the reliability and stable operation of the equipment of technological lines. Welding lines involve, as a rule, special systems using sluice boxes and gears for continuous supply of articles into the welding zone. The high productivity and operation rate of such lines admit stoppage of some units only for a short time. Under these conditions, the plasma emitter electron sources, during the period between two rounds of preventive maintenance of the welding system, performed up to 16,000 welds for fuel elements with zirconium-alloy welds and up to 80,000 welds for those with aluminum-alloy cans. This is 3–5 greater than the number of welds that can be executed by a hot-cathode electron source between two rounds of maintenance.

The experience gained in operating the plasma-emitter electron sources in industrial conditions as units of automatic welding lines has shown that these devices have the following advantages: low sensitivity to the degree of vacuum and to its variations; long lifetime and high reliability, in particular, under the conditions of intense evaporation from the welding bath, and quickness and simplicity of maintenance.

Thus, experience has shown that plasma-emitter electron sources have almost no limitations for operation under conditions typical of electron-beam welding. Moreover, their low sensitivity to the vacuum and gas conditions in the working chamber makes them promising for the development of new welding technologies. In this connection, these devices are currently used to advantage at newly established welding bays and as units of operative equipment instead of hot-cathode guns, providing longer equipment lifetimes and increased the productivity of the welding process.

The ability of the welding plasma-emitter electron sources to operate without taking special measures for protection of the cathode in a wide pressure range under the conditions of

https://doi.org/10.1017/S0263034603212039 Published online by Cambridge University Press

intense gas wastes from the welding zone and their long service life have made possible their efficient use for the production of various coatings by facing with powdered materials (Panin *et al.*, 1999, 2000). The facing process is accompanied, as a rule, by deterioration in vacuum because of the intense gas release in the welding zone, intense sputtering of the powder, and some other processes that call for taking special measures for protection of the hot cathode. The use of plasma-emitter electron sources makes it possible to simplify the electron beam and vacuum equipment, to increase the service life of the source in the period between obligatory preventive maintenance work, and thus make the production of wear-resistive coatings much more economically efficient.

The electron-beam facing has been tested in power production, machine building, petroleum and gas works, metallurgy, and transports and is currently used for the restoration of worn-out and the hardening of new machine parts and tools of various types.

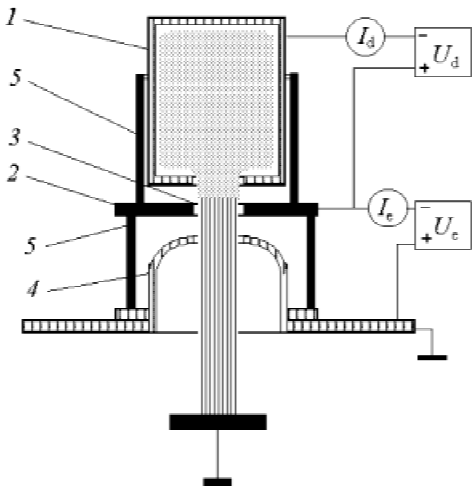


**Fig. 13.** Schematic of an electron source operating in the fore-vacuum pressure range: *1*: hollow cathode, *2*: plane anode, *3*: emission hole, *4*: extraction electrode, and *5*: insulators.

### 2.4. Electron guns for the production of beams in the fore-vacuum pressure range

Some applications of electron beams call for only rough vacuum, which is produced by mechanical pumps. Among these applications are the initiation of chemical and plasma chemical reactions in the gas phase and at the surface and the annealing and melting of materials. The plasma electron sources are attractive for meeting these goals due to their ability to keep the same pressure in the source and in the technological cavity. However, in this case, it is necessary to fulfill two controversial requirements: to create favorable conditions for the ignition of a discharge in the plasma generation region and to prevent the initiation of a discharge (breakdown) in the electron acceleration region. A design of an electron source has been developed (Burdovitsin & Oks, 1999) where this is attained with a combination of a hollow-cathode discharge and a plane-parallel acceleration gap. The source, shown schematically in Figure 13, includes cylindrical hollow cathode *1* of diameter 30 mm and height 60 mm, plane anode *2* with emission hole *3* of 10 mm diameter, and extraction electrode *4* with a central hole of 25 mm diameter.

The emission hole is covered with a metal grid of mesh size 0.5 × 0.5 mm. The device is constructed on cermet insulators *5*. The source is powered from two rectifiers, one connected to the discharge gap and the other to the acceleration gap. The water cooling of the source electrodes makes it possible to increase the discharge current to 1.5 A. In this case, the emission current, that is, the load current of the high-voltage rectifier in continuous operation, is no less than 1 A. The beam current at the collector, placed at a distance of 15 cm from the extractor, makes up over 70% of the emission current at an accelerating voltage of 3–8 kV and a residual gas pressure of 5–13 Pa. The electron beam is divergent; however, when using a system of magnets, it can be focused at the collector to a spot of diameter 5–7 mm. When the collector is removed, a beam discharge occurs in the region where the electron flux density peaks. In this discharge, plasma chemical reactions may proceed, which are accompanied, for instance, by deposition of polymer films if hydrogen is used as the working gas.

Another version of the electron source (Burdovitsin *et al.*, 2002) is intended for the production of a ribbon electron beam. The design of this source is, in fact, a modified version of that considered above. This design uses a long hollow anode of dimensions 300 × 80 × 40 mm. A slit 25 mm wide and 260 mm long is made in the wall facing the anode. In line with this slit, there is a 250 × 10 mm slit in the anode, which is covered with a 0.5 × 0.5 mm metal grid. The acceleration electrode is plane, and its slit is 300 × 40 mm. The electron source being described produces, in continuous operation at a gas pressure of 1.3–8 Pa, a ribbon electron beam (250 × 10 $mm^2$) of energy 2–6 keV and current up to 1 A. In this case, the efficiency of emission, that is, the emission-to-discharge current ratio, is no less than 70%. An important characteristic of a ribbon beam is its linear uniformity. To obtain this characteristic, the current onto a movable probe was measured. Used for the probe was a piece of tungsten wire 1 mm in diameter placed normal to the beam plane at a distance of 2 cm from the acceleration electrode. Typical curves of the collector current distribution are given in Figure 14. The distribution uniformity degrades with increasing gas (air) pressure. However, at a pressure of 8 Pa, the distribution is uniform to within 10%, allowing one to speak of the so produced electron beam for technological purposes.

https://doi.org/10.1017/S0263034603212039 Published online by Cambridge University Press

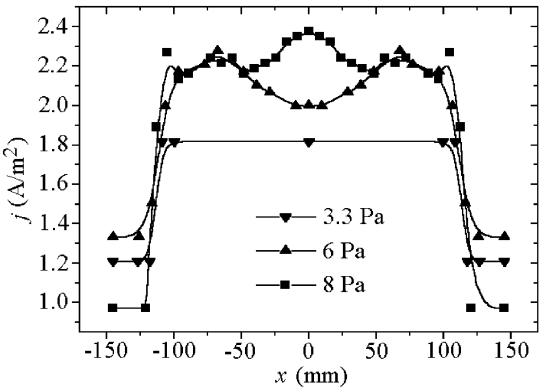


**Fig. 14.** Current density distribution over the beam cross section.

## 3. PLASMA ION SOURCES

### 3.1. The Titan sources and the generation of gas-metal ion beams

The Titan sources have been developed for the modification of the surface properties of materials by irradiating them with charged particle beams. These sources feature the opportunity to produce both gas and metal beams by using two types of arc discharge—constricted and vacuum arcs—in one discharge system. This opens new prospects for the creation in the surface layer of a target of gas–metal compounds showing high strength characteristics. To generate gas ions, a constricted arc discharge with cold cathodes is used. In this type of discharge, the cathode material ions are produced in the cathode region, while plasma is generated in the anode cavity due to the ionization of the working gas. Metal ions are generated during the operation of the cathode spots of a vacuum arc initiated at a cathode made of a desired material. The first prototype of the Titan ion source was developed at the Institute of High Current Electronics more than 10 years ago (Bugaev *et al.*, 1992*b*) and later this ion source was operated at a number of R & D institutions in Russia and abroad. Since that time, several versions of the source have been developed and built, each having special features.

The electrode system of the Titan ion source (Bugaev *et al.*, 1992*c*) is shown in Figure 15. Cold cathodes *1* of the constricted arc, made of magnesium, are located in the discharge chamber into which the working gas flow is supplied. They are arranged one opposite the other on a magnetic core with a magnetic flux created by permanent Sm-Co magnets. The cathodes *1* and loop anode *2* placed between them form a Penning cell. In transfer electrode *3*, there is ferromagnetic insert *4* with a constriction channel at the exit of which cathode *5* of the vacuum arc is placed. The ferromagnetic insert serves as the magnetic core for the "arch"-configured magnetic field created by ring-shaped magnet *6*. Both discharges operate with common hollow anode *7*, which is covered on its emission end face with a fine emission grid.

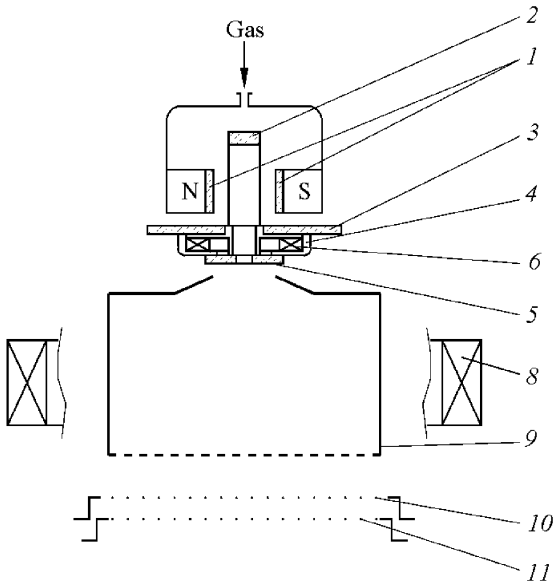


**Fig. 15.** Schematic of the electrode system of the Titan ion source: *1*: constricted arc cathodes, *2*: loop anode, *3*: transfer electrode, *4*: ferromagnetic insert, *5*: vacuum arc cathode, *6*: permanent Sm-Co magnets, *7*: hollow anode, *8*: solenoid, *9*: accelerating electrode, and *10*: intercepting electrode.

Ions are extracted by a dc accelerating voltage of 10–80 kV, which is applied between the hollow anode being at a high positive potential and grounded acceleration electrode *9*. To intercept the secondary electrons knocked out by the ion beam from the collector, a negative voltage of several kilovolts is applied to intercepting electrode *10*. The electrodes *9* and *10* are made of tungsten grids of about 95% transparency. In one version of the source, transverse extraction of a ribbon ion beam through a slit in the lateral wall of a hollow anode was used (Bugaev *et al.*, 1994).

For the Titan source, which operates in the pulsed mode, it is necessary that an arc be stably initiated for a long time, since this process determines the time of continuous operation of the device. The low-current-gas-discharge-based arc-initiating system used in the source has made it possible to lengthen its continuous operation time to a value that depends only on the erosion rate of the cathode material during the operation of the vacuum arc. A version of the Titan ion source has also been developed that operates in the steady-state mode. This device is capable of generating wide-aperture gas and metal ion beams of a current of 100–300 mA.

All versions of the Titan source used various configurations of the magnetic field. In the Titan-2 source, the magnetic field was employed to initiate an auxiliary Penning discharge with permanent magnets arranged on the cathodes of the Penning cell or on the perimeter of the discharge chamber (Nikolaev *et al.*, 1996), while in other versions it was used to improve the source parameters and emission characteristics. Thus, the "arch" magnetic field created in the cathode region of a vacuum arc stabilized the motion of

https://doi.org/10.1017/S0263034603212039 Published online by Cambridge University Press

the cathode spot over the cathode surface (Nikolaev *et al.*, 1998), making the source operation more reliable and the cathode wear more uniform. The 10-mT magnetic field created by solenoid *8*, applied to the anode region, substantially increased the ion extraction efficiency due to the effect of "switching" of the ion current to the emission electrode that appeared as the polarity of the anode layer potential reversed. Moreover, the magnetic field varied the ion current density distribution over the beam cross section.

The design of the last version of the Titan source is shown schematically in Figure 16. Despite the fact that the principle of operation and parameters as well as the system of extraction of the ion beam of this device are the same as those of the prototype (Nikolaev *et al.*, 1996), some units and parts have been changed substantially (Bugaev *et al.*, 2000*b*). Thus, the Titan-3 ion source uses gas insulation to preclude the appearance of carbon and carbide compounds in the ion-alloyed layer of irradiated samples that took place when an oil insulation system was used and the discharge chamber was cooled due to the diffusion of oil through vacuum seals. To do this, dry air or nitrogen is pumped to an excessive pressure of up to 1 atm into grounded air-tight case *4*. Air cooling is used to remove the heat released during the operation of discharges. Provision is made for electrical decoupling *3* of the discharge chamber, being at a high accelerating potential, and the grounded cooling water supply unit. If distilled water is used, this decoupling ensures an appropriate electric strength and low leakage currents at voltages of up to 80 kV. Distilled water circulates in a closed duct cooled with running water. The electric field enhanced at the sharp corners of the discharge chamber was moderated with high-voltage metal screen *7*.

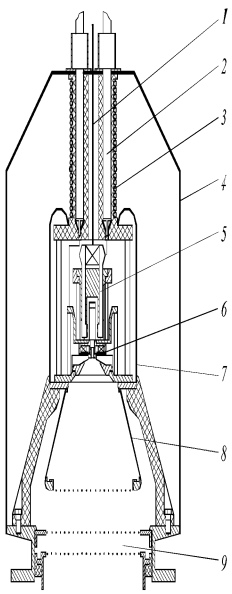


**Fig. 16.** Schematic diagram of the Titan-3 ion source: *1*: pipe for supplying the working gas into the discharge chamber, *2*: high-voltage cable, *3*: pipe for supplying water to cool the discharge chamber, *4*: grounded case, *5*: constricted arc channel, *6*: vacuum arc cathode, *7*: high-voltage screen of the discharge chamber, *8*: hollow anode, and *9*: accelerating and intercepting electrodes.

The constricted discharge is ignited by a high voltage pulse of about 20 $\mu$s duration applied between cathodes *5* and hollow anode *8*. Once an auxiliary discharge has been initiated and a pulsed voltage has been applied to these electrodes, a constricted arc of 20–60 A current and 400 $\mu$s duration starts operating between them. The discharge operation occurring simultaneously with the working gas flow through the constriction channel results in more efficient plasma generation. The gas-discharge plasma fills the hollow anode cavity, and ions are extracted from the developed surface of the cavity, stabilized with an emission grid.

If, once the auxiliary discharge has been initiated, a voltage is applied between cathode *6* and hollow anode *8*, a vacuum arc starts operating between these electrodes with cathode spots formed on the cathode surface. The arc current is 40–150 A and the pulse duration is 400 $\mu$s. During the operation of the vacuum arc, the cathode material plasma coming from the cathode spots fills the hollow anode cavity, and the formation of a metal ion beam occurs similar to that of the gas ion beam from the constricted discharge plasma. The repetition rate of the discharge pulses, and, hence, that of the ion beam can be controlled in the range from 10 to 50 Hz. Since the discharges have independent power supplies and the plasma generation processes in the discharges are different and divorced from each other, it is possible, if the discharges operate simultaneously, to produce a two-component gas–metal ion beam (Fig. 17), the proportion between ion fractions in each component being readily controllable by varying the discharge currents. The total current extracted from the source plasma ranges between 0.1 and 0.3 A for gas ions and from 0.2 to 0.5 A for metal ions.

A total of more than 10 different versions of the Titan source have been designed and built. They are currently operated at the Institute of High Current Electronics, at the technological universities of Dalian and Guangzhou (China), and at Zoltan Institute for Nuclear Research (Poland), where they are used in the main to modify surface properties of materials by the ion implantation method. When doing this,

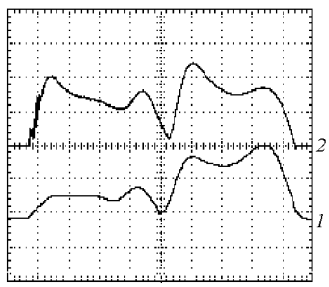


**Fig. 17.** Waveforms of the pulsed currents of the Titan-3 ion source: *1*: discharge current (left: constricted arc, right: vacuum arc, 40 A/div); *2*: ion current (left: nitrogen ions, right: titanium ions, 0.2 A/div). Scale: $\tau$ = 100 мкс/div. $U_{acc}$ = 50 kV.

https://doi.org/10.1017/S0263034603212039 Published online by Cambridge University Press

in the near-surface layer of an article, gas–metal compounds of desired stoichiometry, such as TiN, $Mo_2N$, AlO, and the like, are created that improve the tribological properties of the surface and enhance the corrosion resistance of the article (Tyumentsev *et al.*, 1993). The Titan ion sources were also employed to improve the performance of the electrodes of a gas-discharge laser, to harden cutter knives, stamps, drills, and cutting tools with the aim to lengthen their lifetimes, and to improve the operating characteristics of other articles and tools. An interesting application of the ion source has been found at the University of Zhengzhou (China): The device is used in gene engineering as a tool for the perforation of cells of various biological objects in executing gene variations.

### 3.2. The MEVVA ion source and the generation of multi-charged and gas ions

The ion charge state distribution in the plasma of a vacuum arc discharge is of importance in using this type of discharge primarily for the production of ion beams. Since the energy of an ion in a beam is proportional to its charge, the charge state of the ion beam produced by a technological-purpose source determines the penetration depth of the ions into a solid, the rate of sputtering of the surface layer, and some other parameters. In the ion sources used as injectors of heavy ions for charged particle accelerators, the ion beam charge state is responsible for the fraction of ions participating in further acceleration. For the vacuum arc pulse duration ($>100$ $\mu$s) characteristic of the ion sources depending for their operation on this type of arc, the mean ion charge, depending on the cathode material, varies from 1 to 3. The study of the factors that affect the beam ion charge distribution and the search for ways of increasing the beam ion charge present a problem whose successful solution could offer the prospect for improving vacuum-arc-based ion sources.

The experience gained in developing and operating the Titan ion sources have made it possible to modernize the MEVVA-type ion sources based on a vacuum arc (Oks, 2002) with the aim to increase the ion charge. Figure 18 gives a generalized schematic diagram of this type of ion source. The arc discharge was ignited between cathode *1* and anode *3* as a voltage was applied to the gap from power supply *9*. The ions generated by this discharge were accelerated in multiaperture or grid extraction systems *4* by an accelerating voltage of 10–50 kV (power supply *10*). The ion beam was analyzed with the help of time-of-flight mass spectrometers whose base was the distance between the gate of spectrometer *5* and ion collector *6*. To increase the ion charge, the vacuum arc was subjected to the following actions: (1) a pulsed magnetic field of induction up to 3 T was created in the cathode region of the discharge; (2) an additional current pulse ("step") with an amplitude considerably exceeding the arc current was applied to the discharge gap, and (3) an electron beam with parameters sufficient for efficient ionization ($I_e = 40$ A, $j_e = 70$ A/cm$^2$, $E_e = 20$ keV, $\tau_e = 100$ $\mu$s) was injected into the discharge plasma.

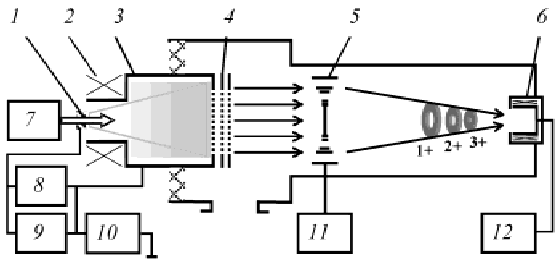


**Fig. 18.** Schematic of the ion source generating multiply charged ions: *1*: cathode, *2*: solenoid, *3*: hollow anode, *4*: acceleration system, *5*: spectrometer gate, *6*: Faraday cup, *7*: electron gun. Power supplies for *8*: arc current "step", *9*: vacuum arc, *10*: accelerating voltage, *11*: spectrometer gate, and *12*: oscilloscope.

The magnetic field created in the plasma of the vacuum arc discharge has a pronounced effect on the ion charge state distribution: The fractions of singly and doubly charged ions substantially decrease, while the multiply charged ion fraction noticeably increases. Comparison of the attained operating voltage of the arc with the ionization potentials has shown that to obtain an appreciable desired degree of ionization, it is necessary that the arc operation voltage be close to the sought-for ionization potential. The ion charge distributions for an arc in a magnetic field for different cathode materials are listed in Table 1. Comparison of these distributions with data obtained in the absence of a magnetic field suggests that for all cathode materials the ion charge increases if a strong magnetic field is created in the discharge gap. As this takes place, the charge number corresponding to the greatest number of ions shifts toward its greater values, and ion species which were not observed earlier ($C^{3+}$, $Ti^{5+}$, $Cr^{5+}$, $Ni^{5+}$, $Ni^{6+}$, $Mo^{6+}$, $Ba^{3+}$, $Ba^{4+}$, $Pb^{3+}$, Hf $^{6+}$, $U^{5+}$, $U^{6+}$, and others) appear in the charge spectrum of the beam. It should be noted that the steady-state ion charge distribution in the plasma of a vacuum arc discharge also depends on the residual gas pressure. To produce an appreciable fraction of metal ions with a charge number over 3+, the residual gas pressure should be lower than $10^{-5}$ Torr.

The charge number of the ion beam generated in a vacuum arc ion source can be increased by applying to the main gap an additional discharge current "step" ($10^2$–$10^3$ A, 5–50 $\mu$s) whose amplitude is considerably greater than that of the main discharge current. On application of such a current step, the voltage across the discharge gap increases. As this takes place, the charge state of the ion beam varies: The fraction of lower-charge ions decreases, while that of higher-charge ions increases, resulting in an increase in the mean ion charge by a factor of 1.2–1.5. If a combination of a magnetic field and a discharge current step is used, the mean charge of the plasma ions can be increased by 10–25%, as compared to the case of the application of a magnetic field only.

https://doi.org/10.1017/S0263034603212039 Published online by Cambridge University Press

**Table 1.** *Ion charge distribution in a beam for different cathode materials with and without a magnetic field in the cathode region. $B = 0.7–3$ T, $I_d = 0.2–1.7$ kA, $p < 10^{-6}$ Torr.*

| | No Magnetic Field | | | | | | With Magnetic Field | | | | | | | |
|---|---|---|---|---|---|---|---|---|---|---|---|---|---|---|
| Cathode | 1+ | 2+ | 3+ | 4+ | 5+ | $\langle Q_0 \rangle$ | 1+ | 2+ | 3+ | 4+ | 5+ | 6+ | $\langle Q \rangle$ | $\frac{\langle Q \rangle}{\langle Q_0 \rangle}$ |
| Li | 100 | — | — | — | — | 1 | 26 | 74 | — | — | — | — | 1.7 | 1.7 |
| C | 100 | — | — | — | — | 1 | 29 | 58 | 13 | — | — | — | 1.8 | 1.8 |
| Mg | 46 | 54 | — | — | — | 1.5 | 1 | 99 | — | — | — | — | 2 | 1.3 |
| Al | 38 | 51 | 11 | — | — | 1.7 | 12 | 55 | 33 | — | — | — | 2.2 | 1.3 |
| Si | 63 | 35 | 2 | — | — | 1.4 | 19 | 51 | 30 | — | — | — | 2.1 | 1.5 |
| Ca | 8 | 91 | 1 | — | — | 1.9 | 10 | 24 | 66 | — | — | — | 2.6 | 1.3 |
| Sc | 27 | 67 | 6 | — | — | 1.6 | 16 | 53 | 29 | 2 | — | — | 2.2 | 1.2 |
| Ti | 11 | 75 | 14 | — | — | 2 | 1 | 9 | 25 | 58 | 7 | — | 3.6 | 1.8 |
| V | 8 | 71 | 20 | 1 | — | 2 | 3 | 8 | 27 | 56 | 6 | — | 3.5 | 1.7 |
| Cr | 10 | 68 | 21 | 1 | — | 2.1 | 4 | 9 | 20 | 53 | 12 | 2 | 3.7 | 1.7 |
| Fe | 25 | 68 | 7 | — | — | 1.8 | 6 | 20 | 34 | 38 | 2 | — | 3.1 | 1.7 |
| Co | 34 | 59 | 7 | — | — | 1.7 | 4 | 17 | 43 | 31 | 5 | — | 3.2 | 1.8 |
| Ni | 30 | 64 | 6 | — | — | 1.8 | 1 | 9 | 19 | 32 | 27 | 12 | 4.1 | 2.3 |
| Cu | 17 | 63 | 20 | — | — | 2 | 10 | 22 | 34 | 31 | 3 | — | 3 | 1.5 |
| Zn | 80 | 20 | — | — | — | 1.2 | 2 | 56 | 34 | 8 | — | — | 2.5 | 2.1 |
| Ge | 60 | 40 | — | — | — | 1.4 | 9 | 28 | 54 | 9 | — | — | 2.6 | 1.9 |
| Sr | 2 | 98 | — | — | — | 2 | 2 | 67 | 21 | 10 | — | — | 2.4 | 1.2 |
| Y | 5 | 62 | 33 | — | — | 2.3 | 6 | 9 | 77 | 8 | — | — | 2.9 | 1.3 |
| Zr | 1 | 47 | 45 | 7 | — | 2.6 | 1 | 11 | 33 | 48 | 7 | — | 3.5 | 1.4 |
| Nb | 1 | 24 | 51 | 22 | 2 | 3 | — | 5 | 8 | 29 | 51 | 7 | 4.5 | 1.5 |
| Mo | 2 | 21 | 49 | 25 | 3 | 3.1 | — | 5 | 12 | 34 | 39 | 10 | 4.4 | 1.4 |
| Rh | 35 | 55 | 7 | 3 | — | 1.8 | 2 | 7 | 27 | 55 | 8 | 1 | 3.6 | 2.0 |
| Pd | 23 | 67 | 9 | 1 | — | 1.9 | 2 | 18 | 48 | 30 | 2 | — | 3.1 | 1.7 |
| Ag | 13 | 61 | 25 | 1 | — | 2.1 | 7 | 23 | 37 | 30 | 3 | — | 3 | 1.4 |
| Cd | 68 | 32 | — | — | — | 1.3 | 5 | 40 | 55 | — | — | — | 2.5 | 1.9 |
| In | 66 | 34 | — | — | — | 1.3 | 10 | 63 | 27 | — | — | — | 2.2 | 1.6 |
| Sn | 47 | 53 | — | — | — | 1.5 | 8 | 61 | 30 | 1 | — | — | 2.2 | 1.5 |
| Ba | 2 | 98 | — | — | — | 2 | — | 42 | 54 | 4 | — | — | 2.6 | 1.3 |
| La | 1 | 76 | 23 | — | — | 2.2 | 3 | 26 | 61 | 10 | — | — | 2.8 | 1.3 |
| Ce | 3 | 83 | 14 | — | — | 2.1 | 1 | 15 | 54 | 27 | 3 | — | 3.2 | 1.5 |
| Pr | 3 | 69 | 28 | — | — | 2.3 | 2 | 20 | 59 | 18 | 1 | — | 3 | 1.3 |
| Nd | — | 83 | 17 | — | — | 2.2 | — | 18 | 36 | 42 | 4 | — | 3.3 | 1.5 |
| Sm | 2 | 83 | 15 | — | — | 2.1 | — | 10 | 40 | 41 | 8 | 1 | 3.5 | 1.7 |
| Gd | 2 | 76 | 22 | — | — | 2.2 | 1 | 28 | 31 | 35 | 5 | — | 3.2 | 1.4 |
| Tb | 2 | 76 | 22 | — | — | 2.2 | 1 | 17 | 39 | 42 | 1 | — | 3.3 | 1.5 |
| Dy | 2 | 66 | 32 | — | — | 2.3 | 2 | 15 | 42 | 39 | 2 | — | 3.2 | 1.4 |
| Ho | 2 | 66 | 32 | — | — | 2.3 | 1 | 13 | 44 | 37 | 5 | — | 3.3 | 1.5 |
| Er | 2 | 63 | 35 | — | — | 2.3 | 1 | 10 | 46 | 35 | 8 | — | 3.4 | 1.5 |
| Hf | 3 | 24 | 51 | 21 | 1 | 2.9 | 1 | 5 | 11 | 39 | 41 | 3 | 4.2 | 1.4 |
| Ta | 2 | 33 | 38 | 24 | 3 | 2.9 | 0 | 4 | 12 | 40 | 41 | 3 | 4.3 | 1.5 |
| W | 3 | 23 | 43 | 26 | 5 | 3.1 | 0 | 1 | 18 | 42 | 32 | 7 | 4.2 | 1.4 |
| Ir | 5 | 37 | 47 | 11 | 1 | 2.7 | 0 | 4 | 22 | 47 | 27 | — | 4 | 1.5 |
| Pt | 13 | 69 | 18 | — | — | 2.1 | 1 | 16 | 42 | 46 | — | — | 3.4 | 1.6 |
| Au | 14 | 75 | 11 | — | — | 2 | 2 | 15 | 38 | 45 | — | — | 3.3 | 1.6 |
| Pb | 36 | 64 | — | — | — | 1.6 | 1 | 65 | 23 | 11 | — | — | 2.4 | 1.5 |
| Bi | 87 | 13 | — | — | — | 1.1 | 7 | 27 | 57 | 9 | — | — | 2.7 | 2.4 |
| Th | — | 24 | 64 | 12 | — | 2.9 | — | 18 | 30 | 26 | 20 | 6 | 3.7 | 1.3 |
| U | 20 | 40 | 32 | 8 | — | 2.3 | — | 19 | 31 | 28 | 18 | 4 | 3.6 | 1.6 |

Injection of an electron beam into the plasma of a vacuum arc discharge also substantially increases the mean ion charge, and the effect of the beam action is more pronounced than that of a strong magnetic field applied for the same purpose. The effect of an electron beam on the ion charge state for a lead cathode is presented in Figure 19. Under conventional conditions of a vacuum arc operating without an injected electron beam, only singly and doubly charged lead ions are detected in the charge spectrum of the plasma (upper trace). An electron beam provides a substantial increase in the fraction of higher charge states (lower trace). With an electron beam, sevenfold ionization of lead was attained. As this took place, the mean charge of the ion beam increased twice: from 1.7 to 3.4. The degree of rise of

https://doi.org/10.1017/S0263034603212039 Published online by Cambridge University Press

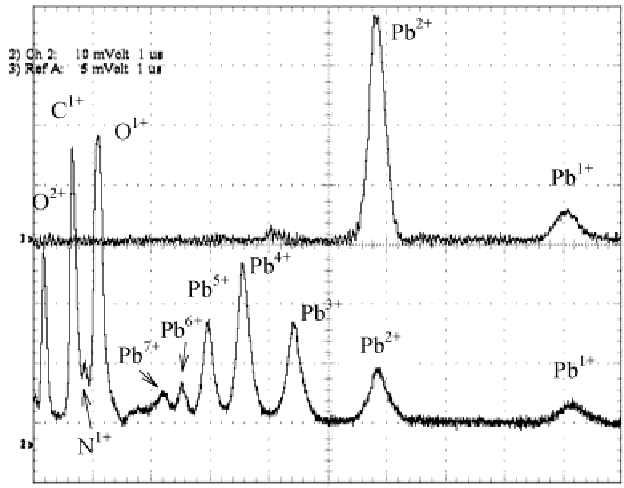


**Fig. 19.** Spectra of a lead ion beam: upper trace: without an electron beam; lower trace: with an electron beam injected into the plasma of the vacuum arc discharge.

the multiply charged ion fraction is determined by the cathode material, the electron beam current and current density, and the pressure of the residual gas or the gas desorbed from the electrodes. To further increase the ion charge, it is necessary to increase the electron beam density and the lifetime of the ions in the region of their interaction with the electron beam and to further reduce the detrimental effect of the gas impurities by decreasing the pressure in the region of interaction of the beam with the ion component of the discharge plasma.

Forced supply of the working gas into the discharge system of a vacuum-arc ion source with a magnetic field allows generation of gas ions and production of two-component "gas–metal" ion beams. Investigations were performed for various working gases and cathode materials that encompassed most of the elements of the periodical table. For all gases and cathode materials used in the experiments, an increase in pressure resulted in a decrease in metal ion current and in multiply charged metal ion fraction in the beam. If a magnetic field was created in the discharge gap, this also gave rise to the appearance in the beam of a considerable fraction of fill gas ions. The process most probably responsible for the variations in the charge of metal ions is the charge exchange of these ions with gas neutrals in the discharge gap. This supposition is supported by numerical estimates based on the relative cross sections of this process determined in the adiabatic approximation. In the presence of a magnetic field and under an elevated pressure, the spectrum of the charge states of metal ions is largely the result of two competing processes: the charge exchange between the ions and residual gas neutrals reducing the mean ion charge and the additional ionization in the magnetic field increasing the fraction of multiply charged ions. The range over which the gas and metal ion fractions in the beam can be controlled in the case of its generation based only a

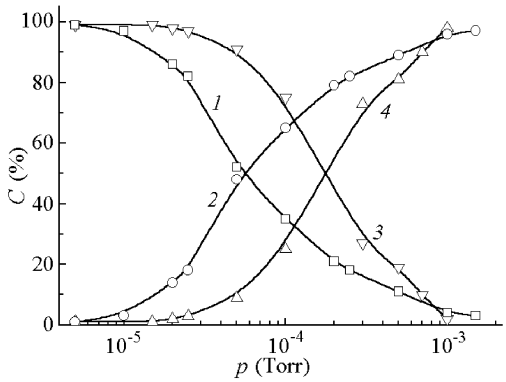


**Fig. 20.** Pressure dependence of the fraction of cathode material ions (*1, 3*) and gas ions (*2, 4*) in the beam. Aluminum (*1*), oxygen (*2*), yttrium (*3*), and nitrogen ions (*4*). $B = 0.1$ T.

vacuum arc discharge in a magnetic field is wider than that in the previously considered case. Figure 20 presents plots of the pressure dependence of the ion content for two cathode material–working gas pairs: aluminum–oxygen and yttrium–nitrogen. From these plots it follows that by varying the gas pressure from $10^{-5}$ to $10^{-3}$ Torr with the amplitude of the pulsed magnetic field kept constant, it is possible to control the oxygen ion content in the ion beam from 0 to 96% and the aluminum ion content, accordingly, from 100 to 4%. For the yttrium cathode and nitrogen, the same variation in pressure controls the nitrogen ion content in the range 0–97% and the yttrium ion content in the range 100–3%. Another way of controlling the proportion between the gas ion and metal ion contents is to vary the magnetic field at a fixed pressure of the working gas. Figure 21 presents the magnetic field dependence of the gas and metal ion contents for cathodes made of yttrium and zirconium and oxygen as the fill gas. By varying the magnetic field from 20 to 200 mT one can control the oxygen ion content in the beam from 5 to 80–85% and the yttrium or zirconium ion content from ~95% to 15%.

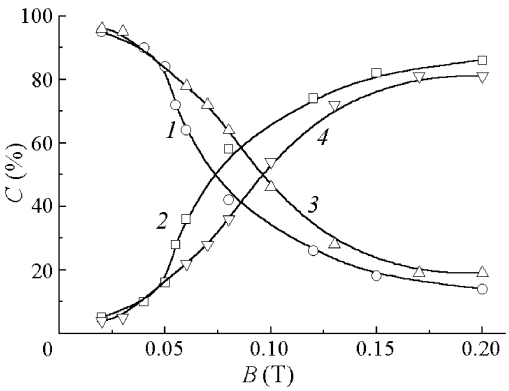


**Fig. 21.** Magnetic field dependence of the fraction of cathode material ions (*1, 3*) and gas ions (*2, 4*) in the beam. Zirconium (*1*) and oxygen ions (*2*) and yttrium (*3*) and oxygen ions (*4*). $p = 6 \cdot 10^{-5}$ Torr.

https://doi.org/10.1017/S0263034603212039 Published online by Cambridge University Press

In contrast to the arc-discharge-based ion sources, which generally operate in the pulsed mode, the glow-discharge-based ion sources are best suited to the generation of continuous beams of gas ions. A glow discharge features highly stable and uniformly distributed parameters of the plasma and a high ion component of the cathode current; therefore, it is workable in various plasma-ion devices. With all its good points, a glow discharge has, however, the disadvantage that its comparatively high (compared, e.g., to an arc discharge) operating voltage, and, hence, intense sputtering of the cathode, reduces the device lifetime and "pollutes" the gas plasma with metal ions of the cathode material. Another factor that limits the use of this type discharge is the rather high operating pressure and its relatively narrow range.

In a glow-type discharge, the principal mechanism of current transfer at the cathode is ion-electron emission. When the mode of a self-sustained low-voltage discharge is realized, the coefficient of ion-electron emission $\gamma$ is generally not above 0.1. It follows that even a small (compared to the discharge current) variation in electronic component of the cathode current may substantially vary the glow discharge parameters, in particular, its operating voltage. This variation can be executed "artificially" by injecting electrons into the discharge system. If conditions for the acceleration of these electrons in the cathode fall of the glow discharge are created, they will be in fact indistinguishable from the electrons emitted by the cathode in the course of ion-electron emission, and this injection of electrons is in effect tantamount to increasing the coefficient of ion-electron emission $\gamma$.

The possibility to vary the quantity $\gamma$ allows either a substantial extension of the operating pressure range of a glow discharge toward the lower pressures or an appreciable decrease in discharge operating voltage under conventional conditions of its realization.

To inject electrons into the cathode region of the main glow discharge, an auxiliary discharge with hollow cathode *1* (Fig. 22) is used whose outlet aperture is arranged opposite the anode, which is made as metal grid *2*. The main discharge with cathode *3* and anode *4* serves to generate plasma from which ions are extracted. The design features of the main discharge gap, depending on the device purpose, allow one to produce either ion beam or gas-discharge plasma in the volume of the discharge chamber. Grid *2* covers the aperture in the wall of the main discharge cathode *3* and is electrically connected to this cathode. Some electrons, which close the auxiliary discharge current, enter the main discharge region through the grid and are accelerated in the cathode fall potential region of this discharge. The accelerated electrons chaotically oscillate between the cavity walls, ionizing the working gas until they are thermalized or get on the discharge anode.

The auxiliary discharge ensures stable initiation of the main discharge with the voltage at its electrodes almost equal to the operating voltage. To initiate the auxiliary discharge, surface dielectric breakdown and an additional magnetron discharge in the magnetic field created by a ring-shaped permanent magnet were used.

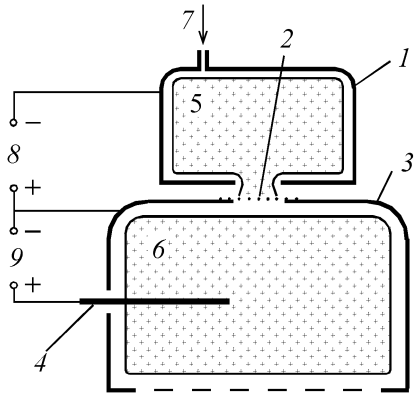


**Fig. 22.** Schematic of the electrode system of the device based on a glow discharge with electron injection: *1*: auxiliary discharge cathode, *2*: metal grid, *3*: main discharge cathode, *4*: main discharge anode, *5*: auxiliary discharge plasma; *6*: main discharge plasma, *7*: gas supply, *8, 9*: power supplies for the main and auxiliary discharges.

The working gas flow is supplied into the cathode cavity of the auxiliary discharge. Estimates show that the pressures in the auxiliary discharge region and in the main discharge region differ by no less than an order of magnitude. The operating pressure is controlled by varying the working gas flow rate.

The shape of the anode *4* (Fig. 22) and its position, in contrast to the surface area, have no effect on the discharge parameters. Measurements have shown (Vizir *et al.*, 2000) that there is an optimum anode-to-cathode area ratio (0.003–0.004) at which the discharge operation pressure and the operating pressure are minimum.

Injection of electrons into the cathode cavity reduces the discharge operation voltage $U$ and makes possible the operation of a low-voltage discharge at lower operating pressures $p$ (Fig. 23; Oks *et al.*, 1998). For a self-sustained discharge (curve *1*), a reduction of the operating pressure to

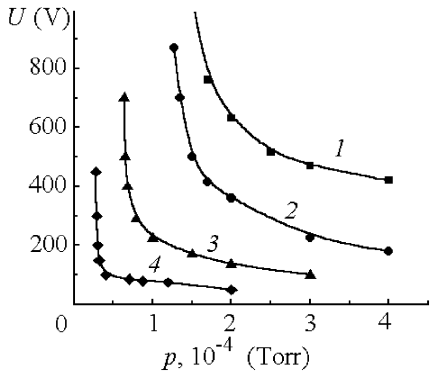


**Fig. 23.** Operating voltage of the main discharge as a function of pressure for different currents of the auxiliary discharge: 0 (*1*), 20 (*2*), 50 (*3*), and 200 mA (*4*). Main discharge current: 100 mA. Working gas: argon.

https://doi.org/10.1017/S0263034603212039 Published online by Cambridge University Press

below $2 \cdot 10^{-4}$ Torr results in an abrupt increase in $U$. As can be seen from the data presented, the electron injection shifts the curves into the region of the lower $U$ and $p$, and the shift magnitude is determined by the injection current.

The injection of electrons is tantamount to increasing the emissive power of the cathode. For an ordinary glow discharge, the coefficient of secondary ion-electron emission is a few percent; therefore, a relatively small fraction of additional electrons is sufficient to change substantially the discharge parameters. Despite the fact that an additional energy should be expended to sustain the auxiliary discharge, the injection of electrons significantly reduces the energy input per ion.

Based on this type of discharge, ion sources has been developed and built that are capable of producing, with an acceleration voltage of up to 30 kV, beams of gas (oxygen inclusive) ions of a cross-sectional area of about 100 $cm^2$ with a current ranging from 1 mA to 2 A (Vizir *et al.*, 2000) as well as plasma generators capable of filling vacuum volumes of about 1 $m^3$ with homogeneous and low-noise gas-discharge plasma of density $3 \cdot 10^{10}$ $cm^3$ with an electron temperature of $T_e = 5$–10 eV.

## 4. CONCLUSION

At the present moment, electron and ion sources based on emission of charge particles from plasma have been developed at many laboratories around the world for electron-beam welding, annealing, surface heating of materials, realizing plasmochemical reactions, ion implantation, or ion-assisted deposition processes. Among the distinctive features of the sources are simplicity, high beam current, and efficiency in producing beams. Since inception, the sources have experienced much improvement in a number of different ways, extending their potential applications. Further improvement in sources technology and an expanding province of novel applications can be expected to be seen in future.

## ACKNOWLEDGMENTS

Research contracts with Lawrence Berkeley and Brookhaven National Laboratories, USA, IPP Trust-I American-Russian scientific cooperation program, CRDF grants GAP # REO-10202-BNL, GAP # REO-10614-LBNL, and BRHE # TO-016-02 are gratefully acknowledged.

## REFERENCES

Belyuk, S.I., Kaplan, A.A., Kreindel, Yu.E. & Rempe, N.G. (1983). High-powered welding electron gun with plasma cathode. In *Plasma-Emitter Electron Sources*, pp. 80–90. Novosibirsk: Nauka. (in Russian).

Bugaev, A., Gushenets, V., Yushkov, G., Oks, E., Kulevoy, T., Hershcovitch, A. & Johnson, B.M. (2001). Electron-beam enhancement of ion charge state fractions in metal-vapor vacuum-arc ion source. *Appl. Phys. Lett.* **79**, 919–921.

Bugaev, A.S., Gushenets, V.I., Khuzeev, Yu.A., Oks, E.M. & Yushkov, G.Yu. (2000*a*). High-density plasma low energy electron gun based on vacuum arc in a strong magnetic fields. *Proc. XIXth Int. Symp. on Discharges and Electrical Insulation in Vacuum*, Vol. 2, pp. 629–632. Xi'an, China: Xi'an Jiaotong University.

Bugaev, A.S., Gushenets, V.I., Nikolaev, A.G., Oks, E.M. & Yushkov, G.Yu. (2000*b*). Future development of gas and metal ion sources based on arc discharge with cold cathode. *Proc. First Int. Congress on Radiation Physics, High Current Electronics and Modification of Materials*, Vol. III, pp. 204–207. Tomsk, Russia. Novosibirsk: Nauka.

Bugaev, S.P., Gushenets, V.I. & Schanin, P.M. (1992*a*). Controlling the emission current from a plasma cathode. *Proc. IXth Int. Conf. on High-Power Particle Beams (BEAMS'92)*, Vol. 2, pp. 1099–1105. Washington, DC, USA: University of Maryland.

Bugaev, S.P., Nikolaev, A.G., Oks, E.M., Schanin, P.M. & Yushkov, G.Yu. (1992*b*). The 100 kV gas and metal ion source for a high current ion implantation. *Rev. Sci. Instrum.* **63**, 2422–2424.

Bugaev, S.P., Nikolaev, A.G., Oks, E.M., Schanin, P.M. & Yushkov, G.Yu. (1992*c*). Improvement of the emission parameters in the "TITAN" vacuum-arc ion source. *Proc. XVth Int. Symp. on Discharges and Electrical Insulation in Vacuum*, pp. 686–689. Darmstadt, Germany.

Bugaev, S.P., Nikolaev, A.G., Oks, E.M., Schanin, P.M. & Yushkov, G.Yu. (1994). The "TITAN" Ion Source. *Rev. Sci. Instrum.* **65**, 3119–3125.

Burdovitsin, V. & Oks, E. (1999). Hollow cathode plasma electron gun for beam generational forepump gas pressure. *Rev. Sci. Instrum.* **70**, 2975–2978.

Burdovitsin, V.A., Burachevsky, Yu.A., Fedorov, M.V. & Oks, E.M. (2002). Plasma electron source of linear beam for forvacuum pressure range. *Proc. 6th Int. Conf. on Modification of Materials with Particle Beams and Plasma Flows*, pp. 57–60. Tomsk, Russia: Tomsk Polytechnic University.

Galansky, V.L., Gruzdev, V.A., Osipov, I.V. & Rempe, N.G. (1994). Physical processes in plasma electron emitters based on a hollow-cathode reflected discharge. *J. Phys. D: Appl. Phys.* **27**, 953–961.

Gavrilov, N.V., Gushenets, V.I., Koval, N.N., Oks, E.M., Tolkachev, V.S. & Schanin, P.M. (1993). Large cross section plasma cathode electron sources. In *Plasma Emitters of Charged Particle*, pp. 42–78. Ekaterinburg: Nauka.

Gielkens, S.W.A., Peters, P.J.M., Witteman, W.J., Borovikov, P.V., Stepanov, A.V., Tskhai, V.M., Zavijalov, M.A., Guschenets, V.I. & Koval, N.N. (1996). A long-pulse 300 keV electron gun with a plasma cathode for high-pressure gas lasers. *Rev. Sci. Instrum.* **67**, 2449–2452.

Gilmour, A.S., Jr. & Lockwood, D.L. (1972). Pulsed Metallic-Plasma Generators. *Proc. IEEE* **60**, 977–991.

Gushenets, V.I. & Schanin, P.M. (1999). Formation of hollow-cathode nanosecond high current glow discharge. *Proc. XXIVth Int. Conf. on Phenomenon in Ionized Gases*, Vol. II, pp. 201–202. Warsaw, Poland.

Gushenets, V.I., Koval, N.N. & Schanin, P.M. (1986). High current electron accelerator with plasma cathode. *Proc. VIth All-Union Symp. on High-Current Electronics*, part 2, pp. 112–114. Tomsk, USSR.

Gushenets, V.I., Koval, N.N., Kuznetsov, D.L., Mesyats, G.A., Novoselov, Yu.N., Uvarin, V.V. & Schanin, P.M.

(1991). High-frequency generation of large-cross-section pulsed electron beams. *Pisma Zh. Tekh. Fiz.* **17**, 834–836.

Gushenets, V.I., Koval, N.N., Tolkachev, V.S. & Schanin, P.M. (1999). Nanosecond high current and high repetition rate electron source. *IEEE Trans. Plasma Sci.* **27**, 1055–1059.

Gushenets, V.I., Oks, E.M., Yushkov, G.Yu. & Rempe, N.G. (2003). Current status of plasma emission electronics: I. Basic physical processes. *Laser Part. Beams* **21**, 123–137.

Koval, N.N., Kreindel, Yu.E., Mesiats, G.N., Tolkachev, V.S. & Schanin, P.M. (1983). Efficiency use of low pressure arc in the plasma electron emitter. *Pisma Zh. Tekh. Fiz.* **9**, 568–572.

Koval, N.N., Kreindel, Yu.E., Tolkachev, V.S. & Schanin, P.M. (1985). The effect of gas on development of a vacuum arc with a hollow anode. *IEEE Trans. Electr. Insul.* **20**, 735–737.

Kozyrev, A.V., Korolev, Yu.D. & Shemiakin, I.A. (1994). Processes in cathode region of low pressure arc discharge. *Izv. Vyssh. Ucheb. Zaved., Fizika,* No. 3, 5–25.

Nazarenko, O.K., Kaydalov, A.A. & Kovbasenko, S.N. (1987). *Electron-Beam Welding*. (Paton, B.E., Ed.). Kiev: Naukova Dumka (in Russian).

Nikolaev, A.G., Oks, E.M., Schanin, P.M. & Yushkov, G.Yu. (1996). Vacuum arc/metal ion sources with a magnetic field. *Rev. Sci. Instrum.* **67**, 1213–1215.

Nikolaev, A.G., Oks, E.M., Yushkov, G.Yu., MacGill, R., Discinson, M. & Brown, I.G. (1998). Processes involved in vacuum arc triggering by ExB discharge. *Proc. XVIIIth Int. Symp. on Discharges and Electrical Insulation in Vacuum*, Vol. I, pp. 101–104. Eindhoven, Netherlands: The Institute of Electrical and Electronics Engineers.

Oks, E.M. (2002). Generation of multiple charged ions in vacuum arc plasmas. *IEEE Trans. Plasma Sci.* **30**, 2068–2073.

Oks, E.M., Visir, A.V. & Yushkov, G.Yu. (1998). Low pressure hollow cathode glow discharge plasma for broad beam gaseous io source. *Rev. Sci. Instrum.* **69**, 853–855.

Oks, E. & Yushkov, G. (1996). Some features of vacuum arc plasmas with increasing gas pressure in discharge gap. *Proc. XVII Int. Symp. on Discharges and Electrical Insulation in Vacuum*, Vol. II, pp. 584–588. Berkeley, CA, USA: The Institute of Electrical and Electronics Engineers.

Panin, V.E., Belyuk, S.I., Durakov, V.G., Pribytkov, G.A. & Rempe, N.G. (1999). Electron beam facing of powdered materials. *Proc. Third Int. Symp. SIBCONVERS'99*, Vol. 2, pp. 548–550. Tomsk, Russia: Tomsk University of Control System and Radioelectronics.

Panin, V.E., Belyuk, S.I., Durakov, V.G., Pribytkov, G.A. & Rempe, N.G. (2000). Electron beam facing in vacuum: equipment, technology, coating properties. *Svarochnoe Proizvodstvo* No. 2, 34–38.

Rempe, N. & Osipov, I. (2000). A plasma-cathode electron source designed for industrial use. *Rev. Sci. Instrum.* **71**, 1638–1641.

Rempe, N.G., Osipov, I.V. & Troyan, O.E. (2000). Gun with plasma cathode for electron beam welding. *Proc. Int. Conf. on Welded Structures*, pp. 119–120. Kiev, Ukraine.

Spadtke, P., Emig, H., Wolf, B.H. & Oks, E. (1994). Influence of gas added to MEVVA discharge on the extracted ion beam. *Rev. Sci. Instrum.* **65**, 3113–3118.

Tyumentsev, A.N., Pinzhin, Yu.P., Korotaev, A.D., Behert, A.E., Savchenko, A.O., Kolobov, Yu.R., Bugaev, S.P., Schanin, P.M. & Yushkov, G.Yu. (1993). Phase transformations in Mo under simultaneous implantation of metal and gas ions. *Nucl. Instrum. Meth. Phys. Res. B* **80/81**, 491–495.

Vintizenko, L.G., Gushenets, V.I., Koval, N.N., Koval, G.A., Mesyats, G.A., Skakun, V.S., Tarasenko, V.F., Fedenev, A.V. & Schanin, P.M. (1986). Lasing in inert gases with pumping by the electron beam of an accelerator with a plasma cathode. *Dokl. AN SSSR* **31**, 431–433.

Vintizenko, L.G., Gushenets, V.I., Koval, N.N., Tolkachev, V.S. & Schanin, P.M. (1988). Convergent electron beam accelerator with plasma cathode. *Proc. Seventh Int. Conf. on High-Power Particle Beams (BEAMS'88)*, pp. 1491–1496. Karlsruhe: Kernforschungszentrum.

Vizir, A.V., Yushkov, G.Yu. & Oks, E.M. (2000). Further development of a gaseous ion source based on low-pressure hollow cathode glow. *Rev. Sci. Instrum.* **71**, 728–730.

Volkov, A.A., Pchelkin, R.D. & Rempe, N.G. (2001). Stability of parameters of electron sources with plasma emitter in multiple facing mode of operation. *Svarochnoe Proizvodstvo* No. 1, 23–28.